ELSEVIER

Journal of Organometallic Chemistry 510 (1996) 243–253

Journal of Organometallic Chemistry

Molecular structure of some [1.1]ferrocenylruthenocenophanium^{n+} ($n = 1, 2$) polyiodides salts

Masanobu Watanabe [a,*], Izumi Motoyama [a], Hirotoshi Sano [b]

[a] Department of Chemistry, Faculty of Engineering, Kanagawa University, Rokkakubashi, Yokohama 221, Japan
[b] Department of Chemistry, Faculty of Science, Tokyo Metropolitan University, Minami-ohsawa, Hachioji, Tokyo 192-03, Japan

Received 19 July 1995

Abstract

Oxidation of [1.1]ferrocenylruthenocenophane with a large excess and 1.5 equivalents of iodine gives dicationic iodo[1.1]ferrocenylruthenocenophanium^{2+} $I_3^- \cdot 0.5(I_3^-)_2 \cdot 0.5I_2$ (**1**) and monocationic [1.1]ferrocenylruthenocenophanium$^+$ I_3^- (**2**) salts respectively. The structures of **1** and **2** were analyzed by single-crystal X-ray diffraction studies. The crystal form of **1** is monoclinic space group $C2/c$, $a = 21.351(5)$, $b = 20.594(5)$, $c = 17.397(4)$ Å, $\beta = 124.17(1)°$, $Z = 8$, and the final $R = 0.068$ and $R_w = 0.070$. The cation formulated as $[Fe^{III}(C_5H_4CH_2C_5H_4)_2Ru^{IV}I]^{2+}$ exists in a *syn*-conformation as in the cases of the neutral compound. The distance between the Ru^{IV} and Fe^{II} is 4.656(4) Å, which is much shorter than the value of the neutral compound (4.792(2) Å), and the bond angle of $I–Ru^{IV} \cdots Fe^{III}$ is 81.26°. The dihedral angle between the two η^5-C_5H_4 (fulvenide) rings on the Ru^{IV} moiety is 37.56° due to the Ru^{IV}–I bond (2.758(3) Å). These two rings of Fe^{III} and Ru^{IV} moieties are essentially eclipsed. The unit cell has three kinds of I_3^- (I_{3a}^-, I_{3b}^- and I_{3c}^-) and one I_2, and the formula of **1** is given as $[Fe^{III}(C_5H_4CH_2C_5H_4)_2Ru^{IV}I]^{2+}I_3^- \cdot 0.5(I_3^-)_2 \cdot 0.5I_2$. The crystal of **2** formulated as $[Fe^{III}(C_5H_4CH_2C_5H_4)_2Ru^{II}]^+I_3^-$ is triclinic space group $P\bar{1}$, $a = 13.487(6)$, $b = 15.404(7)$, $c = 11.458(4)$ Å, $\alpha = 95.59(3)°$, $\beta = 101.00(3)°$ $\gamma = 79.38(3)°$, $Z = 2$, and the final $R = 0.067$ and $R_w = 0.068$. The unit cell has two independent molecules (unit A and B); i.e. two kinds of distance between the Ru^{II} and Fe^{III} are observed; one (**A**) is 4.615(3) and the other (**B**) is 4.647(3) Å. The two η^5-C_5H_4 rings of both Fe^{III} and Ru^{II} are essentially staggered and the dihedral angles between the rings of FcH and RcH moieties are less than 5.8°. Typical ferrocenium-type broad singlet ^{57}Fe-Mössbauer lines are observed for both salts (**1**, **2**) at all temperatures.

Keywords: Iron; Ruthenium; Metallocenes; Ferrocene

1. Introduction

[1.1]ferrocenylruthenocenophane is an interesting molecule because ferrocene (FcH) and ruthenocene (RcH) are bridged by a $-CH_2-$ group in *syn*-conformation. Therefore some intramolecular interaction between Fe and Ru atoms will be expected. Recently we reported an X-ray analysis study on the oxidation product (**3**) of [1.1]ferrocenylruthenocenophane with iodoruthenocenium$^+$ BF_4^- ($[RcHI]^+BF_4^-$). On the basis of the results of the X-ray analysis of **3**, the cation is formulated as $[Fe(C_5H_4CH_2C_5H_4)_2RuI]^+$ and the two η^5-C_5H_4 rings in the RcH moiety are largely slanted (the dihedral angle between the rings is 33.87°) due to the Ru–I bond (2.751(1) Å) [1], as shown in Fig. 1. One of the interesting structural features of the salt is a twisted $C_5H_4CH_2C_5H_4$ ligand: i.e. one has a large twisted angle (42.02°) and the other has a small one (11.19°), probably because of electrostatic interaction between the BF_4^- and the cation $[Fe(C_5H_4CH_2C_5H_4)_2RuI]^+$ (from the unit cell projection, the cation is directed to the BF_4^-). The distance between the Ru and Fe is 4.719(1) Å, which is shorter than the corresponding value of the neutral compound (4.792(2) Å) [2]. All the results indicate clearly that the oxidation states of the Fe and Ru atoms in the cation are Fe^{II} and Ru^{IV} respectively, and the cation is formulated as $[Fe^{II}(C_5H_4CH_2C_5H_4)_2Ru^{IV}I]^+$. The result is contrary to cyclic voltammogram results on [1.1]ferrocenylruthenocenophane; i.e. the study shows two independent peaks: a quasi-reversible one-electron oxidation peak ascribed to $Fe^{II} \rightarrow Fe^{III}$ at 400 mV, and an irreversible two-electron oxidation peak to $Ru^{II} \rightarrow Ru^{IV}$ at 940 mV [3] (i.e. the Fe atom is oxidized easily). In the present study, oxidation of [1.1]ferrocenylruthenocenophane with iodine was carried out; i.e. oxidation with a large excess of iodine

* Corresponding author.

SSDI 0022-328X(95)05919-9

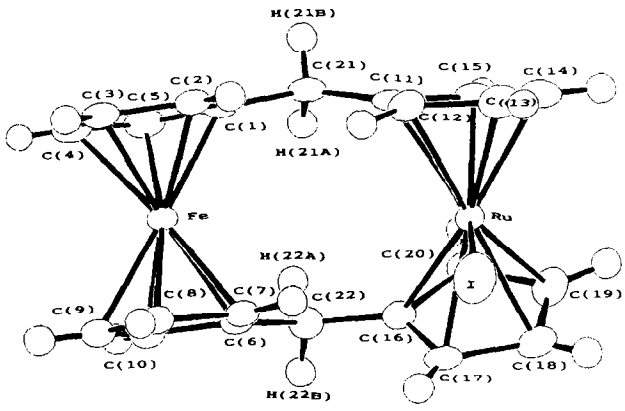

Fig. 1. ORTEP drawing of cation 3.

gave a dicationic salt **1** and with 1.5 equivalent amount of iodine gave a monocationic salt **2**. The aim of the present study is to investigate the crystal structures of **1** and **2** in comparison with those of the original compound and **3** and to discuss the different oxidation mechanism of [1.1]ferrocenylruthenocenophane with I_2 and with $[RcHI]^+$.

2. Experimental

2.1. Syntheses

Salt **1** was prepared as follows: [1.1]Ferrocenylruthenocenophane (100 mg, 0.227 mmol; prepared by reduction of [1.1]ferrocenylruthenocenophane-1,13-dione with $LiAlH_4$ and $AlCl_3$ according to the method reported previously [4]) dissolved in 50 cm^3 of benzene was added to a large excess of iodine (500 mg, 1.97 mmol) dissolved in 100 cm^3 of benzene. The mixture was stirred for 10 min. Black precipitates were formed. Salt **1** was obtained by recrystallization from a CH_3CN–$C_2H_5OC_2H_5$ mixture as black crystals (280 mg; yield 85%). Single crystals were obtained by the following method. Salt **1** was dissolved in CH_3CN. To this solution, ether was carefully diffused for a few days. The single crystals were formed on the side of the container at room temperature. Anal. Found: C, 18.45; H, 1.30. $C_{22}H_{20}FeI_8Ru$. Calc.: C, 18.14; H, 1.38%. Salt and single crystals of **2** were prepared by a similar method as for **1**, using 1.5 equivalent of I_2 ([1.1]ferrocenylruthenocenophane; 100 mg, 0.227 mmol and I_2; 86.5 mg, 0.341 mmol). Anal. Found: C, 31.98; H, 2.35. $C_{22}H_{20}FeI_3Ru$. Calc.: C, 32.15; H, 2.45%.

2.2. Measurements

^{57}Fe-Mössbauer measurements were carried out using a ^{57}Co(Rh) source moving in a constant acceleration mode. The isomer shift values were referred to metallic iron foil. The Mössbauer parameters were obtained by least-squares fitting to Lorentzian peaks. The experimental error of the isomer shifts and quadrupole splitting values was ± 0.02 mm s^{-1}. The ^{13}C CP/MAS

Table 1
Crystal and intensity collection data for **1**,**2**

	Compound	
	1	**2**
Formula	$C_{22}H_{20}FeI_8Ru$	$C_{44}H_{40}Fe_2I_6Ru_2$
Formula weight	1456.55	1644.06
Space group	$C2/c$	$P\bar{1}$
a (Å)	21.351(5)	13.487(6)
b (Å)	20.594(5)	15.404(7)
c (Å)	17.397(4)	11.458(4)
α (°)	90.0	95.59(3)
β (°)	124.17(1)	101.00(3)
γ (°)	90.0	79.38(3)
V (Å^3)	6329(2)	2291(1)
Z	8	2
Dx (g cm^{-3})	3.06	2.38
T (°C)	23	23
λ (Å)	0.71073	0.71073
μ (cm^{-1})	87.54	106.8
No. of reflections measured	7662	10375
No. of observed reflections	3290 ($I > 2\sigma(I)$)	5253 ($I > 2\sigma(I)$)
R [a]	0.068	0.067
R_w [b]	0.070	0.068

[a] $R = \Sigma \| |F_o| - |F_c| \| / \Sigma |F_o|$.
[b] $R_w = (\Sigma\omega(\| |F_o| - |F_c| \|^2 / \Sigma\omega(|F_o|^2))^{1/2}$.

NMR measurements were carried out by the same method reported previously [1].

2.3. X-ray crystallography

Crystals ($0.1 \times 0.1 \times 0.3$ mm^3) of **1**, ($0.1 \times 0.4 \times 0.2$ mm^3) of **2** were selected. X-ray diffraction experiments were carried out on a Rigaku AFC-6A automated four-circle X-ray diffractometer with graphite monochromatized Mo-K α radiation ($\lambda = 0.71073$ Å). The intensity data were collected at $25 \pm 1°$ using the 2θ–ω scan mode with a scanning speed of 4° min^{-1}. The lattice parameters were determined by a least-squares calculation with 25 reflections. Crystal stability was checked by recording three standard reflections every 150 reflections, and no significant variations were observed. For **1**, 7662 reflections were collected in the range $2\theta \leq 55°$, 7465 were unique ($R_{int} = 0.04$), of which 3042 reflections with $I_{obsd} > 2\sigma$ (I_{obsd}) were used for the structure determination. The scan width was $1.21 + 0.3 \tan \theta$. The refinement 291 variable parameters converged to $R = \Sigma \| F_o | - | F_c \| / \Sigma | F_o | = 0.067$, $R_w = [\Sigma \omega (| F_o | - | F_c |)^2 / \Sigma \omega F_o^2]^{1/2} = 0.061$. For **2**, 10375 reflections were collected in the range $2\theta \leq 55°$, 9950 were unique ($R_{int} = 0.027$), of which 5253 reflections with $I_{obsd} > 2\sigma$ (I_{obsd}) were used for the structure determination. The scan width was $1.42 + 0.3 \tan \theta$. The refinement 457 variable parameters converged to $R = 0.068$, $R_w = 0.066$.

The non-hydrogen atoms were refined anisotropically by full matrix least squares. Hydrogen atoms were fixed at the calculated positions. Neutral atom scattering factors were taken from Cromer and Waber [5] and anomalous dispersion effect corrections were included in F_c. The values of $\Delta f'$ and $\Delta f''$ were those of Creagh and McAuley [6]. All of the calculations were performed using the TEXSAN crystallographic software package [7]. Crystallographic data for **1** and **2** and some of the

Table 2
Selected bond lengths and angles of **1**, **2** and related compounds

	1	2		3	[1.1]Ferrocenoruthenocenophane
		A	B		
Fe–Ru	4.656(4)	4.615(3)	4.647(3)	4.719(1)	4.792(2)
Fe–Cp [a]	1.706(6)	1.684(10)	1.711(5)	1.654(2)	1.665(7)
Ru–Cp [b]	1.824(2)	1.794(2)	1.803(5)	1.861(8)	1.788(5)
Fe–C_{ring} (av)	2.08(4)	2.07(4)	2.09(4)	2.047(6)	2.055(6)
Ru–C_{ring} (av)	2.21(4)	2.15(2)	2.16(3)	2.22(3)	2.151(6)
Ru–I	2.758(3)			2.751(1)	
C_{ring}–C_{ring} (Fe)	1.41(3)	1.40(6)	1.41(4)	1.42(1)	
C_{ring}–C_{ring} (Ru)	1.39(3)	1.37(9)	1.42(5)	1.42(3)	
Bond angles (°)					
I–Ru · · · Fe	81.26			91.50	
C(1)–C(21)–C(11)	124.2(9)	130.5(8)	121.5(6)	121.0(5)	120.4(5)
C(6)–C(22)–C(16)	113.6(8)	114.2(9)	117.8(5)	119.0(5)	120.7(5)

Dihedral angles between planes (°) for 1

	Plane		
	C(6)–C(10)	C(11)–C(15)	C(16)–C(20)
C(1 ~ 5)	5.54	17.24	20.43
C(6 ~ 10)	—	12.24	25.87
C(11 ~ 15)	—	—	37.56

Dihedral angles between planes (°) for 2

Plane (unit **A**)	Plane		
	C(6)–C(10)	C(11)–C(15)	C(16)–C(20)
C(1)–C(5)	5.64	30.38	30.10
C(6)–C(10)	—	32.26	32.55
C(11)–C(15)	—	—	3.19
Plane (unit **B**)	Plane		
	C(28)–C(32)	C(33)–C(37)	C(38)–C(42)
C(23)–C(27)	5.77	30.11	31.98
C(28)–C(32)	—	30.02	32.09
C(33)–C(37)	—	—	2.23

[a] Fe–Cp; the distance between the Fe and η^5-Cp and η^5-C_5H_4 rings.
[b] Ru–Cp; the distance between the Ru and η^5-Cp and η^5-C_5H_4 rings.

experimental conditions for the X-ray structure analysis are listed in Table 1.

3. Results and discussion

3.1. Salt 1

The final atomic coordinates and equivalent isotropic temperature factors (B_{eq}) of non-hydrogen atoms, interatomic distances, and selected bond lengths and angles for **1** are shown in Tables 2, 3 and 4. ORTEP drawings of the cation with the atomic numbering system are shown in Fig. 2. The conformation of the cation is similar to that of reported cation **3** formulation as $[Fe^{II}(C_5H_4CH_2C_5H_4)_2Ru^{IV}I]^+$; i.e. the cation exits in a *syn*-conformation and the iodine atom is coordinated to the Ru from the opposite side of the methylene group. The Ru–I distance (2.758(3) Å) corresponds well with the reported Ru^{IV}–I value (2.751(1) Å) of **3** [1]. The distances from I(1) to C(12), C(13), C(17) and C(18) are found to be 3.16(2), 3.29(3), 3.18(3) and 3.30(3) Å respectively. These values are much smaller than the sum (3.85 Å) of van der Waals radii of C and I atoms [8], therefore a large dihedral angle (37.56°) between the two η^5-C_5H_4 rings is found in the RcH moiety, which is larger than the corresponding values for **3** (33.87°) and $[RcHI]^+I_3^-$ (32.2°) [1,9]. The interplane C(15) · · · C(20), C(14) · · · C(19), C(13) · · · C(18), C(12) · · · C(17) and C(11) · · · C(16) distances are found to be 2.93(3), 3.13(3), 3.95(3), 4.26(3) and 3.62(3) Å respectively. The largest C(12) · · · C(17) distance is longer than the corresponding value of $[RcHI]^+I_3^-$ (4.11(3) Å) [9]) because of a larger dihedral angle between the η^5-C_5H_4 planes of **1**. However, the rings of the FcH moiety are nearly parallel (the dihedral angle between the planes is 5.54°). The average interplane $C_{ring} \cdots C_{ring}$ distance of the FcH moiety is found to be 3.41(9) Å. The Fe(1) · · · Ru(1) distance is found to be 4.656(4) Å (which is slightly shorter than the value for **3** (4.719(1) Å)).

As shown in Fig. 2, the η^5-C_5H_4 rings of each FcH and RcH moiety are essentially eclipsed as in the case

Table 3
Atomic coordinates ($\times 10^4$) and isotropic temperature factors (Å^2) for **1**

Atom	x	y	z	B_{eq} [a] (Å^2)
I(1)	1530.6(12)	2377.1(9)	5432.3(15)	5.0
I(2)	4382.7(11)	51.2(9)	6016.8(13)	4.3
I(3)	3575.8(11)	688.1(8)	4274.5(14)	4.0
I(4)	2632.3(18)	1264.3(11)	2341.8(16)	8.2
I(5) [b]	0	3234.2(15)	2500	7.2
I(6) [b]	0	1857.1(14)	2500	5.0
I(7) [b]	0	404.8(15)	2500	6.1
I(8)	1055.8(11)	1375.9(11)	−474.6(14)	4.8
I(9) [b]	0	1444.1(13)	−2500	3.7
I(10)	4357.8(18)	1526.3(12)	2505.0(17)	8.4
Ru(1)	1670.3(11)	1046.5(10)	5638.3(14)	2.6
Fe(1)	3200.9(19)	1631.5(18)	8758.7(24)	2.8
C(1)	2138(12)	1186(11)	8286(16)	2.5
C(2)	2036(15)	1874(13)	8119(19)	3.8
C(3)	2532(15)	2181(13)	9016(18)	3.5
C(4)	2891(15)	1711(15)	9675(17)	3.8
C(5)	2679(12)	1092(13)	9261(17)	3.0
C(6)	3689(12)	1278(13)	8052(17)	3.1
C(7)	3542(14)	1948(12)	7889(19)	3.1
C(8)	3930(16)	2264(13)	8744(21)	3.9
C(9)	4342(17)	1831(16)	9457(22)	4.7
C(10)	4202(15)	1202(14)	9065(21)	3.9
C(11)	1289(12)	760(11)	6574(16)	2.4
C(12)	883(13)	1288(12)	6079(17)	3.1
C(13)	455(12)	1116(18)	5080(17)	4.6
C(14)	633(17)	483(15)	5034(22)	4.4
C(15)	1132(15)	246(13)	5903(19)	3.9
C(16)	2919(12)	794(11)	6438(16)	2.4
C(17)	2776(14)	1322(13)	5868(19)	3.7
C(18)	2211(15)	1160(13)	4884(18)	3.5
C(19)	2036(15)	514(15)	4901(18)	3.9
C(20)	2456(14)	292(11)	5803(18)	2.9
C(21)	1720(15)	658(13)	7593(19)	3.7
C(22)	3477(13)	678(12)	7457(16)	2.8

[a] $B_{eq} = 4/3(B_{11}a^2 + B_{22}b^2 + B_{33}c^2 + B_{13}ac \cos \beta)$. B_{ij}s are defined by $\exp[-(h^2B_{11} + k^2B_{22} + l^2B_{33} + 2klB_{23} + 2hlB_{13} + 2hkB_{12})]$.
[b] Site occupation factor $p = 0.5$.

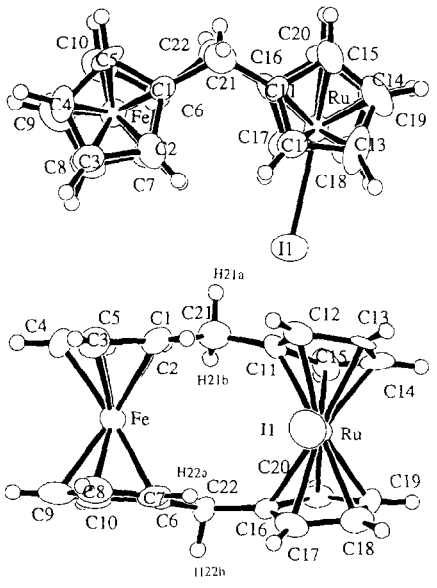

Fig. 2. ORTEP drawing of $[IRu^{IV}(C_5H_4CH_2C_5H_4)_2Fe^{III}]^{2+}$ cation with the numbering scheme of the atoms.

of RcH and $[RcHI]^+$ cation; i.e. the two η^5-C_5H_4 rings rotate about 2.8° for FcH and 1.0° for RcH moieties (the rotation angle is 0° for the precisely eclipsed and 36.0° for the exactly staggered conformation). The average Cp–ring C_{ring}–C_{ring} bond lengths of the FcH and RcH moieties are 1.41(3) and 1.39(4) Å respectively. Both values agree with that of the reported FcH (1.403 ± 0.02 Å [10]) and RcH (1.43(3) Å [11]). However, the mean Fe–C_{ring} distance (2.08(4) Å) is larger than that obtained for FcH (2.045 ± 0.01 Å) and the neutral compound (2.055(6) Å [2]) and closer to that of ferrocenium (FcH^+; 2.075 Å) [11]. The mean Ru–C_{ring} distance (2.21(4) Å) is also larger than the corresponding value for the neutral compound (2.151(6) Å) and closer to the values for **3** (2.22(3) Å) and $[RcRcI]^+$ cation (2.22(2) Å) [1,13]. Furthermore, the distances from the Fe and Ru to the least-squares mean planes of the two η^5-C_5H_4 rings (Fe–Cp, Ru–Cp; see (Table 2) are 1.706(6) and 1.824(2) Å respectively. Both values are closer to those for FcH^+ (1.70 Å) and $[RcHI]^+$ (1.84 Å [9]) respectively. Therefore oxidation states of Fe and Ru atoms are estimated as Fe^{III} and Ru^{IV} and the cation is formulated as $[Fe^{III}(C_5H_4CH_2C_5H_4)_2Ru^{IV}I]^+$ in the solid considering the results of elemental analysis data.

^{57}Fe-Mössbauer spectroscopic study of **1** supports this conclusion; i.e. a temperature independent typical ferrocenium type broader singlet peak (isomer shifts; 0.52 mm s^{-1} at 78 K and 0.48 mm s^{-1} at 300 K) was observed at all the temperatures. Although several ^{13}C-CP/MAS NMR peaks were observed for **3** [1], no clear ^{13}C-CP/MAS NMR signals were observed for **1** because of its paramagnetism (Fe^{III}).

The C(1)–C(21)–C(11) and C(6)–C(22)–C(16) an-

Table 4
Selected interatomic distances for **1**

Atom 1	Atom 2	Distance (Å)	Atom 1	Atom 2	Distance (Å)
Ru(1)	I(1)	2.758(3)	Fe(1)	Ru(1)	4.656(4)
Fe(1)	I(1)	5.036(4)	I(2)	I(3)	2.830(3)
I(3)	I(4)	3.027(3)	I(5)	I(6)	2.836(4)
I(6)	I(7)	2.991(4)	I(8)	I(9)	2.932(2)
I(10)	I(10)	2.752(7)	Fe(1)	C(1)	2.14(2)
Fe(1)	C(2)	2.14(3)	Fe(1)	C(3)	2.06(2)
Fe(1)	C(4)	2.05(2)	Fe(1)	C(5)	2.08(2)
Fe(1)	C(6)	2.14(2)	Fe(1)	C(7)	2.12(2)
Fe(1)	C(8)	2.04(2)	Fe(1)	C(9)	2.06(3)
Fe(1)	C(10)	2.09(3)	Ru(1)	C(11)	2.27(2)
Ru(1)	C(12)	2.26(2)	Ru(1)	C(13)	2.21(2)
Ru(1)	C(14)	2.18(3)	Ru(1)	C(15)	2.20(3)
Ru(1)	C(16)	2.27(2)	Ru(1)	C(17)	2.24(2)
Ru(1)	C(18)	2.19(2)	Ru(1)	C(19)	2.14(2)
Ru(1)	C(20)	2.18(2)	C(1)	C(2)	1.44(3)
C(1)	C(5)	1.43(3)	C(1)	C(21)	1.49(3)
C(2)	C(3)	1.45(4)	C(3)	C(4)	1.36(3)
C(4)	C(5)	1.41(4)	C(6)	C(7)	1.41(3)
C(6)	C(10)	1.47(4)	C(6)	C(22)	1.51(4)
C(7)	C(8)	1.39(4)	C(8)	C(9)	1.37(4)
C(9)	C(10)	1.42(4)	C(11)	C(12)	1.36(3)
C(11)	C(15)	1.47(3)	C(11)	C(21)	1.48(3)
C(12)	C(13)	1.48(3)	C(13)	C(14)	1.37(4)
C(14)	C(15)	1.36(4)	C(16)	C(17)	1.39(3)
C(16)	C(20)	1.43(3)	C(16)	C(22)	1.50(3)
C(17)	C(18)	1.48(4)	C(18)	C(19)	1.39(4)
C(19)	C(20)	1.38(3)			

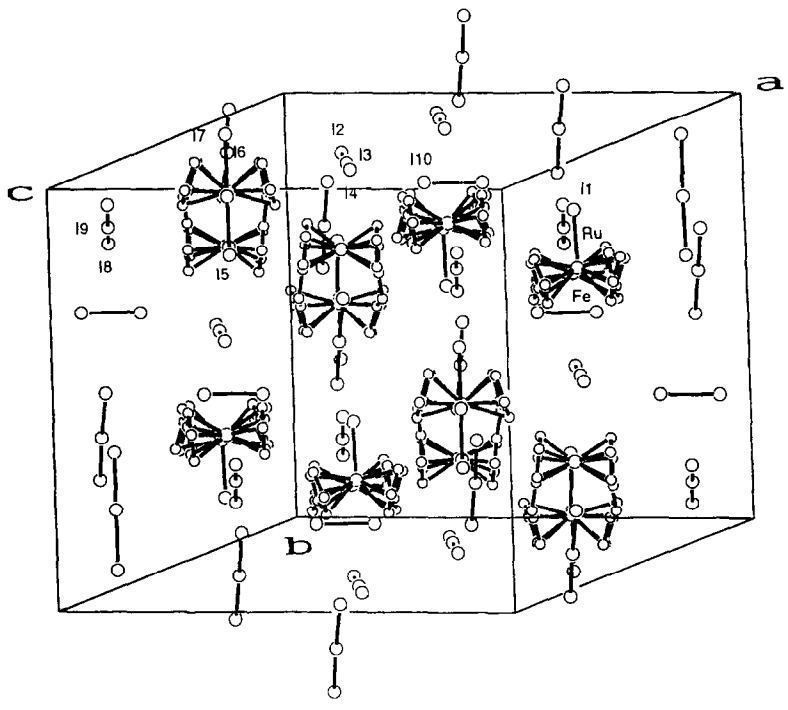

Fig. 3. Projection of the unit cell of **1**.

gles are found to be 124.2(9) and 113.6(8)° respectively, these are closer to the values for the neutral compound (120.4(5) and 120.7(5)° [2]) and **3** (121.0(5) and 119.0(5)° [1]). One of the differing points of structure of **1** compared with **3** is the twisted structure of the $C_5H_4CH_2C_5H_4$ system; i.e. an anomalously large twisted angle (42.02°) is observed for **3** between the planes C(6 ~ 10) and C(16 ~ 20) (11.19° between the planes C(1 ~ 5) and C(11 ~ 15)), as described in the Introduction. For **1**, two relatively closer kinds of twisted angle are observed (12.24° between the planes C(1 ~ 5) and C(11 ~ 15); and 25.87° between the planes C(6 ~ 10) and C(16 ~ 20)).

A stereo view of the packing ($Z = 8$) and the view down the c axis of **1** are shown in Figs. 3 and 4 respectively. The cations are aligned along the a and b axes. The shortest intermolecular C · · · C distance in the cation is 3.30(5) Å (C(14) · · · C(14)*). This value is smaller than the sum of the van der Waals radii of two C atoms (3.40 Å) [8], hence the cations at near van

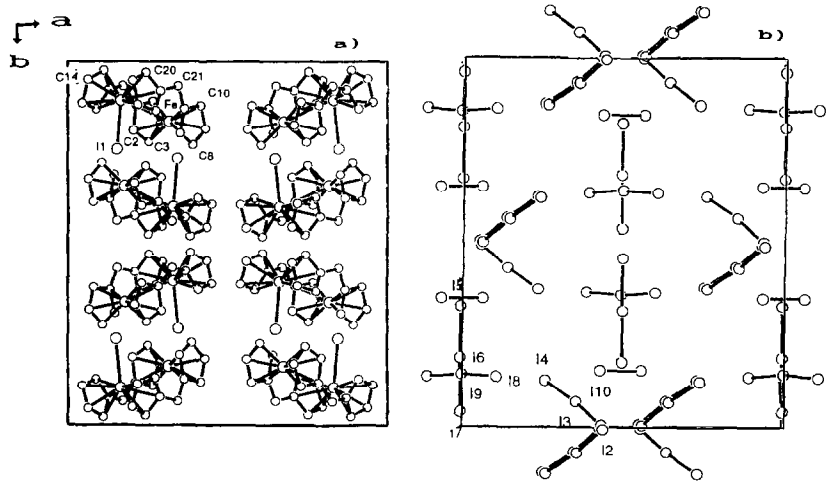

Fig. 4. Projection of the unit cell of **1** along the c axis. (a) $[IRu^{IV}(C_5H_4CH_2C_5H_4)_2Fe^{III}]^{2+}$ cation; (b) I_3^- anion (I_{3a}^-: I2–I3–I4; I_{3b}^-: I5–I6–I7; I_{3c}^-: I8–I9–I8*; I_2: I10–I10*).

der Waals contact to each other. The shortest intermolecular I(1) · · · I(1) distance is 5.161(5) Å, therefore there is no interaction between them. The I(1) sits towards the Fe atoms, but the shortest intermolecular distance (7.90 Å) between them shows clearly no interaction. The unit cell has three independent asymmetric I_3^- anions (I(2)–I(3)–I(4): I_{3a}^-; I(5)–I(6)–I(7): I_{3b}^-; I(8)–I(9)–I(8)*; I_{3c}^-) and one kind of I_2 (I(10)–I(10)*), as

Table 5
Atomic coordinates ($\times 10^4$) and isotropic temperature factors (Å^2) for **2**

Atom	x	y	z	B_{eq} [a] (Å^2)
I(1)	−178.5(15)	4294.6(15)	−7141.5(21)	9.3
I(2)	1692.2(12)	3820.0(9)	−5424.6(15)	6.3
I(3)	3611.5(13)	3342.7(14)	−3816.5(19)	8.5
I(4)	5864.4(13)	2123.3(11)	−1772.4(15)	6.8
I(5)	7672.5(13)	1488.6(9)	−48.8(13)	6.2
I(6)	9492.9(15)	792.9(12)	1675.0(16)	7.4
Ru(1)	6610.0(12)	−4637.8(11)	8829.7(15)	4.5
Ru(2)	3006.4(11)	−43.5(9)	5792.2(13)	3.5
Fe(1)	8017.5(24)	−2094.9(17)	9837.8(23)	4.8
Fe(2)	2080.0(18)	−2828.4(16)	4964.5(24)	3.7
C(1)	8391(22)	−3017(15)	1136(18)	2.5
C(2)	9184(28)	−2999(19)	563(23)	10.9
C(3)	9487(23)	−2254(25)	754(26)	11.8
C(4)	8839(23)	−1618(17)	1392(22)	9.2
C(5)	8178(23)	−2173(17)	1621(19)	8.4
C(6)	6580(17)	−2126(11)	8717(17)	5.2
C(7)	7367(16)	−2494(11)	8097(17)	5.2
C(8)	8029(16)	−1834(16)	8095(18)	6.7
C(9)	7644(17)	−1064(14)	8723(20)	6.9
C(10)	6771(15)	−1170(14)	9099(21)	6.8
C(11)	7876(18)	−4647(21)	248(22)	9.6
C(12)	8252(16)	−4716(18)	9271(25)	7.9
C(13)	8065(17)	−5432(12)	8583(23)	6.8
C(14)	7569(17)	−5863(15)	9201(27)	8.6
C(15)	7419(21)	−5379(21)	289(27)	10.5
C(16)	5614(14)	−3417(13)	8511(18)	5.0
C(17)	5088(14)	−3884(14)	9045(17)	5.1
C(18)	5005(15)	−4736(15)	9303(22)	6.2
C(19)	5400(13)	−4692(13)	7289(19)	5.5
C(20)	5787(14)	−3820(11)	7372(17)	4.2
C(21)	7975(15)	−3870(18)	1232(30)	10.5
C(22)	5680(15)	−2420(12)	8925(19)	5.2
C(23)	3650(13)	−2814(12)	5535(18)	4.8
C(24)	3498(14)	−3396(12)	4515(20)	5.1
C(25)	3007(15)	−4067(14)	4841(21)	6.3
C(26)	2839(16)	−3842(17)	5992(22)	6.8
C(27)	3242(13)	−3110(13)	6438(19)	5.3
C(28)	1250(11)	−1697(10)	4038(16)	3.6
C(29)	984(15)	−2540(16)	3476(20)	6.5
C(30)	568(15)	−2978(12)	4229(21)	5.6
C(31)	602(21)	−2440(21)	5287(22)	6.3
C(32)	1008(13)	−1641(13)	8511(18)	5.0
C(33)	4024(14)	−1241(14)	6372(17)	4.5
C(34)	3316(15)	−1013(14)	7138(15)	5.1
C(35)	3391(13)	−208(14)	7696(18)	6.0
C(36)	4158(18)	−171(16)	7324(23)	7.7
C(37)	4588(13)	−514(13)	6502(20)	5.2
C(38)	1946(12)	−243(9)	4132(14)	3.3
C(39)	1443(14)	314(14)	4957(17)	4.9
C(40)	1899(15)	1137(11)	5205(18)	4.8
C(41)	2698(14)	1031(11)	4582(18)	4.8
C(42)	2722(15)	164(14)	3906(17)	5.2
C(43)	4260(14)	−2088(12)	1515(18)	4.8
C(44)	1674(14)	−1105(15)	3442(16)	5.5

[a] $B_{eq} = 4/3(B_{11}a^2 + B_{22}b^2 + B_{33}c^2 + B_{13}ac\cos\beta + B_{12}ab\cos\gamma + B_{23}bc\cos\alpha)$. B_{ij}s are defined by $\exp[-(h^2B_{11} + k^2B_{22} + l^2B_{33} + 2klB_{23} + 2hlB_{13} + 2hkB_{12})]$.

shown in Fig. 4(b). I_{3b}^- is parallel to the *b* axis and I_{3c}^- and I_2 are parallel to the *a* axis. The I–I distances are found to be 2.830(3)(I(2)–I(3)), 3.027(3)(I(3)–I(4)), 2.836(4) (I(5)–I(6)), 2.991(4)(I(6)–I(7)), 2.932(2) (I(8)–I(9)), 2.752(7) (I(10)–I(10)*) Å. These values are in accordance with that for the reported I_3^- ions [13] and I_2. The bond angles of I–I–I are found to be 175.2° for I_{3a}^-, 180.0° for I_{3b}^- and 174.6° for I_{3c}^-. The former two I_3^- anions are I_2–I^- character, where the I(4) and I(7) atoms carry more negative charge than the other I atoms (I(2), I(3), I(5) and I(6)). The distances of the I(1) · · · I(3), I(1) · · · I(4) and I(1) · · · I(6) are 4.040(3), 4.271(3) and 4.377(2) Å respectively. These are less than or closer to the sum (4.30 Å) of van der Waals radii of two I atoms [8]; i.e. I(1) is near van der Waals contact to the I_{3a}^- and I_{3b}^-. Avoiding steric hindrance between them, I(1) may be located close to the Fe(1) atom. Actually, a much smaller I(1)–Ru(1) · · · Fe(1) bond angle (81.26°) and Fe(1) · · · I(1) distance (5.036(4) Å) are observed compared with the corresponding values for **3** (91.50° and 5.524(1) Å). The I_{3a}^- anion is also near van der Waals contact to the I_{3c}^- and I_2 because the distance I(4) · · · I(8) and I(4) · · · I(10) are found to be 4.107(3) and 3.573(5) Å. All the results show clearly

Table 6
Selected interatomic distances for **2**

Atom 1	Atom 2	Distance (Å)	Atom 1	Atom 2	Distance (Å)
I(1)	I(2)	2.909(2)	I(2)	I(3)	2.895(2)
I(4)	I(5)	2.909(2)	I(5)	I(6)	2.944(2)
Fe(1)	Ru(1)	4.615(3)	Fe(2)	Ru(2)	4.647(3)
Fe(1)	C(1)	2.08(2)	Fe(1)	C(2)	2.01(3)
Fe(1)	C(3)	2.04(3)	Fe(1)	C(4)	2.06(3)
Fe(1)	C(5)	2.03(2)	Fe(1)	C(6)	2.12(2)
Fe(1)	C(7)	2.10(2)	Fe(1)	C(8)	2.08(2)
Fe(1)	C(9)	2.07(2)	Fe(1)	C(10)	2.09(2)
Fe(2)	C(23)	2.10(2)	Fe(2)	C(24)	2.09(2)
Fe(2)	C(25)	2.09(3)	Fe(2)	C(26)	2.05(2)
Fe(2)	C(27)	2.09(2)	Fe(2)	C(28)	2.15(2)
Fe(2)	C(29)	2.06(2)	Fe(2)	C(30)	2.10(2)
Fe(2)	C(31)	2.07(2)	Fe(2)	C(32)	2.14(2)
Ru(1)	C(11)	2.12(2)	Ru(1)	C(12)	2.16(2)
Ru(1)	C(13)	2.16(2)	Ru(1)	C(14)	2.11(2)
Ru(1)	C(15)	2.12(3)	Ru(1)	C(16)	2.12(2)
Ru(1)	C(17)	2.21(2)	Ru(1)	C(18)	2.16(2)
Ru(1)	C(19)	2.17(2)	Ru(1)	C(20)	2.19(2)
Ru(2)	C(33)	2.17(2)	Ru(2)	C(34)	2.18(2)
Ru(2)	C(35)	2.17(2)	Ru(2)	C(36)	2.15(2)
Ru(2)	C(37)	2.15(2)	Ru(2)	C(38)	2.18(2)
Ru(2)	C(39)	2.14(2)	Ru(2)	C(40)	2.20(2)
Ru(2)	C(41)	2.19(2)	Ru(2)	C(42)	2.17(2)
C(1)	C(2)	1.36(5)	C(1)	C(5)	1.35(4)
C(1)	C(21)	1.55(3)	C(2)	C(3)	1.24(5)
C(3)	C(4)	1.44(5)	C(4)	C(5)	1.44(4)
C(6)	C(7)	1.39(3)	C(6)	C(10)	1.56(3)
C(7)	C(8)	1.47(3)	C(8)	C(9)	1.40(3)
C(9)	C(10)	1.35(4)	C(11)	C(12)	1.32(4)
C(11)	C(15)	1.39(5)	C(11)	C(21)	1.55(4)
C(12)	C(13)	1.32(3)	C(13)	C(14)	1.33(4)
C(14)	C(15)	1.38(5)	C(16)	C(17)	1.34(3)
C(17)	C(18)	1.51(3)	C(18)	C(19)	1.38(3)
C(19)	C(20)	1.53(3)	C(23)	C(24)	1.41(3)
C(23)	C(27)	1.41(3)	C(23)	C(43)	1.49(3)
C(24)	C(25)	1.45(3)	C(25)	C(26)	1.38(4)
C(26)	C(27)	1.34(3)	C(28)	C(29)	1.48(3)
C(28)	C(32)	1.39(3)	C(28)	C(44)	1.43(3)
C(29)	C(30)	1.38(3)	C(30)	C(31)	1.40(3)
C(31)	C(32)	1.47(3)	C(33)	C(34)	1.40(3)
C(33)	C(37)	1.44(3)	C(33)	C(43)	1.51(3)
C(34)	C(43)	1.51(3)	C(34)	C(35)	1.34(3)
C(35)	C(36)	1.43(4)	C(36)	C(37)	1.46(3)
C(38)	C(39)	1.39(3)	C(38)	C(42)	1.38(2)
C(38)	C(44)	1.55(3)	C(39)	C(40)	1.50(3)
C(40)	C(41)	1.38(3)	C(41)	C(42)	1.48(2)

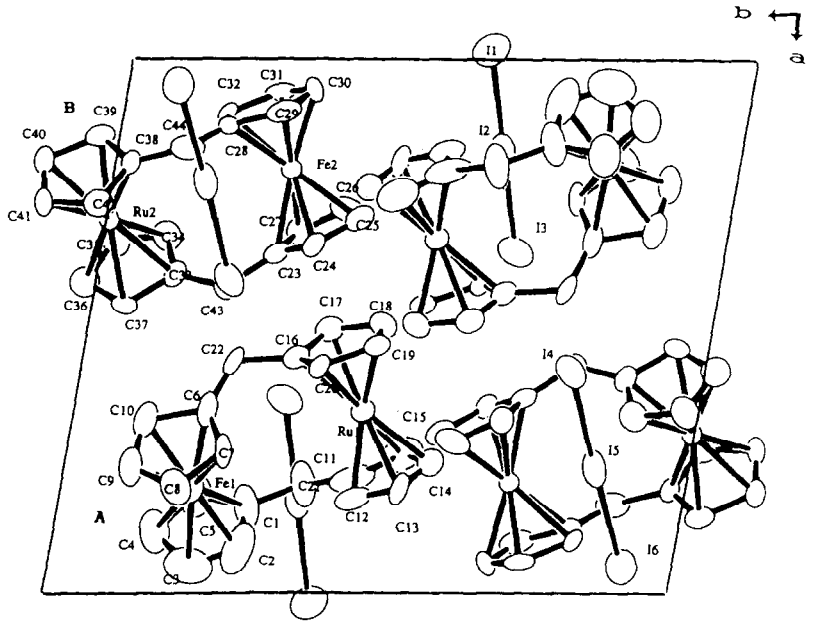

Fig. 5. Projection of the unit cell of **2** along the *a* axis.

that **1** is formulated as $[Fe^{III}(C_5H_4CH_2C_5H_4)_2$-$Ru^{IV}I]^+I_3^- \cdot 0.5(I_3^-)_2 \cdot 0.5I_2$.

3.2. Salt 2

The final atomic coordinate and equivalent isotropic temperature factors (B_{eq}) of non-hydrogen atoms, selected interatomic distance, selected bond lengths and angles for **2** are shown in Tables 5, 6 and 2, and a stereo view of the packing as viewed down the *c* axis is shown in Fig. 5. Two metallocene moieties are inequivalent (unit **A**, **B**) in the triclinic unit cell. Although the basic molecular structure of cation **A** (Fe(1)Ru(1)) is similar to that of cation **B** (Fe(2)Ru(2)), the two cations differ only slightly in detail. Mean Fe(1)–C_{ring}, Ru(1)–C_{ring} and C_{ring}–C_{ring} distances of cation **A** are 2.07(4), 2.15(2), 1.40(6) (FcH moiety) and 1.37(9) Å (RcH moiety) respectively, which correspond well to the equivalent values of cation **B** (2.09(4), 2.16(3), 1.41(4) and 1.42(5) Å, respectively). The distances from the Ru(1) and Fe(1) to the least-squares mean planes (η^5-C_5H_4) are 1.794(2) and 1.684(10) Å respectively, and the values of Ru(2) and Fe(2) moiety are 1.803(5) and 1.711(5) Å respectively.

Although all the lengths (Ru–C_{ring} and Ru–Cp) of the RcH moiety correspond well to the equivalent values of RcH moiety in the [1.1]ferrocenylruthenocenophane, the values of the FcH moiety are longer than the values of the FcH moiety in the neutral compound (see Table 2) and are closer to those of FcH^+ [11]. Therefore oxidation states of both Ru and Fe atoms are estimated as Ru^{II} and Fe^{III} respectively, and the salt **2** is formulated as $[Fe^{III}(C_5H_4CH_2C_5H_4)_2$-$Ru^{II}]^+I_3^-$ considering the results of elemental analysis data. The results of the ^{57}Fe-Mössbauer and ^{13}C-CP/MAS spectroscopies of **2** support the conclusion; i.e. temperature independent broader typical ferrocenium singlet line (I. S., 0.51 at 78 K and 0.32 mm s^{-1} at 300 K) and no ^{13}C-NMR signals were observed.

The two η^5-C_5H_4 planes of Fe^{III} and Ru^{II} moieties are nearly parallel (the dihedral angle between them is less than 5.8°, as shown in Table 2). Although the two η^5-C_5H_4 rings of each FcH and RcH moiety of **1** are essentially eclipsed, those of **2** are staggered; i.e. the

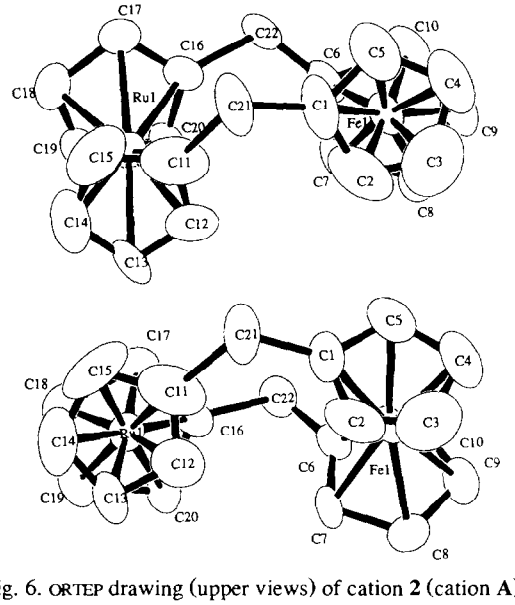

Fig. 6. ORTEP drawing (upper views) of cation **2** (cation **A**).

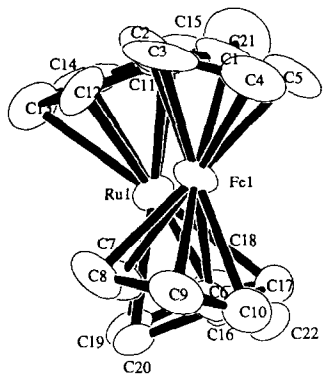

Fig. 7. ORTEP drawing (side views) of cation **2** (cation **A**).

rotation angles of the rings are 23.8° (Fe^{III}) and 31.0° (Ru^{II}) for cation **A** and 28.8° and 29.0° respectively for cation **B**, see Fig. 6.

There are two types of I_3^- anion (I(1)–I(2)–I(3); I_{3a}^- and I(4)–I(5)–I(6); I_{3b}^-). The I–I distances are found to be 2.909(2) (I(1)–I(2)), 2.895(2) (I(2)–I(3)), 2.909(2) (I(4)–I(5)), 2.944(2) (I(5)–I(6)) Å and the bond angles of I–I–I are found to be 177.1(1) for I_{3a}^-, 178.3(1)° for I_{3b}^-. The shortest intermolecular I · · · I distance is 3.779(3) Å (I(3) · · · I(4)), which is much shorter than the sum (4.30 Å) of the van der Waals radii of I. Therefore the I_3^- sit at van der Waals contact to each other. The distances of I(1) · · · C(11), I(1) · · · C(21), I(2) · · · C(7) and I(6) · · · C(32) are found to be 3.85(2), 3.77(3), 3.81(2) and 3.86(2) Å respectively. These values are less than or closer to the value (3.85 Å) of the sum of the van der Waals radii of I and C. Therefore the I_3^- sits at van der Waals contact to the cation, as shown in Fig. 5. Thus the large twisted structure of the $C_5H_4CH_2C_5H_4$ system should be caused by the repulsion between them. Actually, large twisted angles between the planes C(1 ~ 5)–C(11 ~ 15), C(6 ~ 10)–C(16 ~ 20) are observed at 30.38 and 32.55° respectively, for cation **A** (see Fig. 7) and at 30.11 and 32.09° for cation **B**. These values are much larger than the values for the neutral compound (17.6 and 16.7°) and **1** (12.24 and 25.87°). The largely twisted structure of the $C_5H_4CH_2C_5H_4$ system (see Fig. 7) gives a staggered conformation of η^5-C_5H_4 planes (described formerly, see Fig. 6) and much shorter Fe · · · Ru distances (4.615(3) Å for cation **A** and 4.647(3) Å for cation **B**) compared with the value of the original compound (4.792(2) Å).

4. Conclusions

From the results obtained in the present study, it has been found that the oxidation of [1.1]ferrocenylruthenocenophane with 1.5 equivalent of I_2 gives a monocationic salt **2** formulated as $[Fe^{III}(C_5H_4CH_2C_5H_4)_2Ru^{II}]^+I_3^-$ and an excess of I_2 gives a dicationic salt **1** formulated as $[Fe^{III}(C_5H_4CH_2C_5H_4)_2Ru^{IV}I]^{+}\cdot I_3^- \cdot 0.5(I_3^-)_2 \cdot 0.5I_2$ with the Ru^{IV}–I. The result is in accordance with that from cyclic voltammograms. However, the oxidation of [1.1]ferrocenylruthenocenophane with an equivalent amount of $[RcHI]^+BF_4^-$ gives a monocationic salt **3** formulated as $[Fe^{II}(C_5H_4CH_2C_5$-

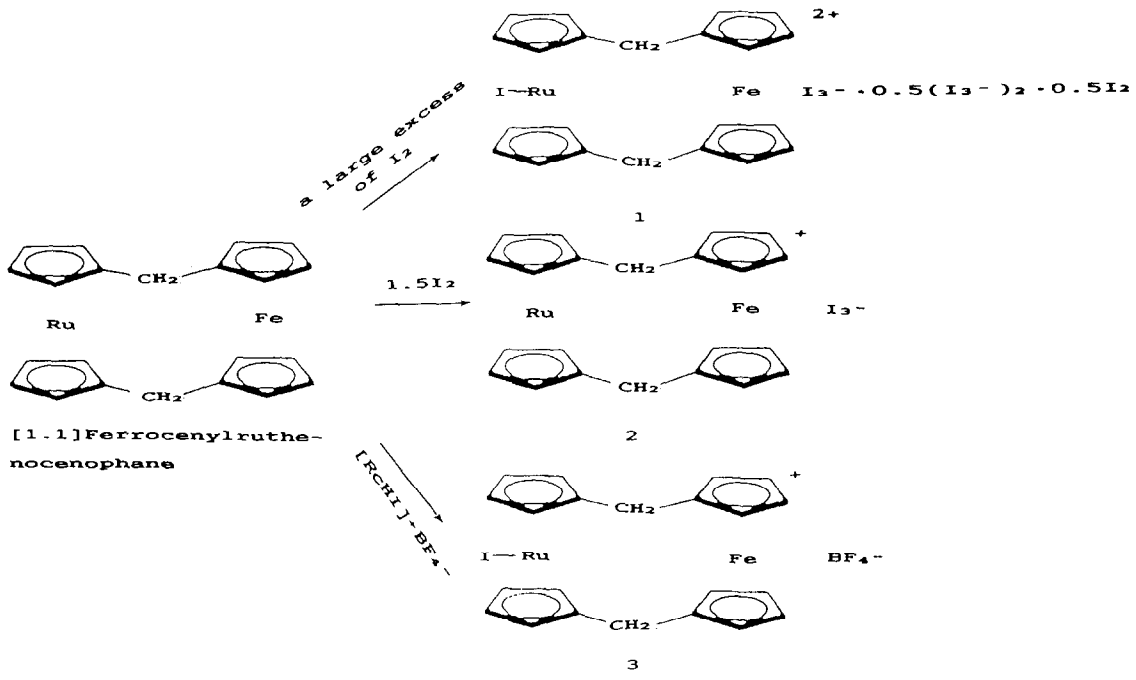

Scheme 1.

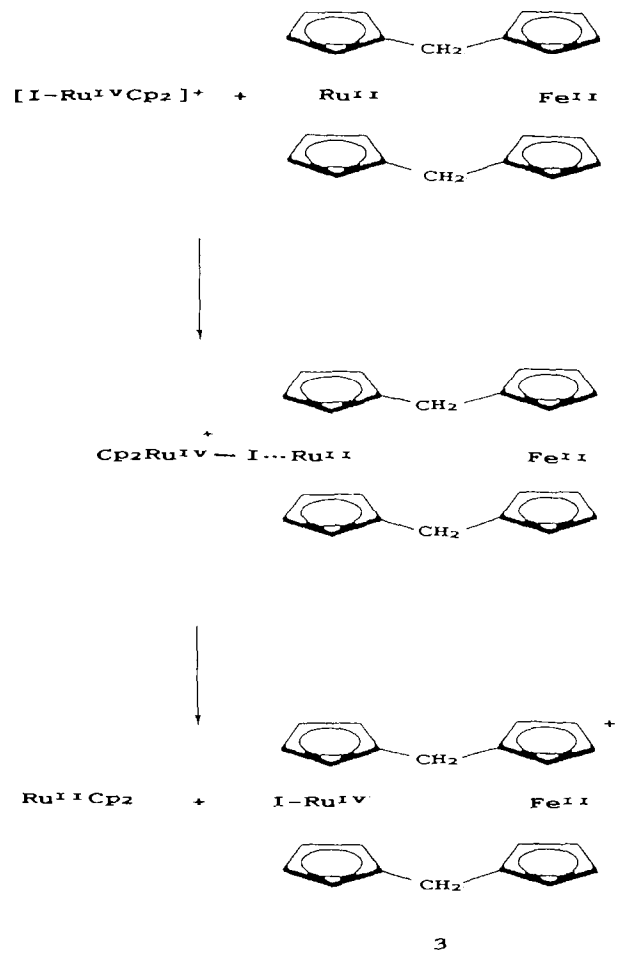

Scheme 2.

$H_4)_2Ru^{IV}I]^+BF_4^-$, not a monocationic $[Fe^{III}(C_5H_4CH_2$-$C_5H_4)_2Ru^{II}]^+BF_4^-$ ferrocenium salt, as shown in Scheme 1.

Recently, the present authors, Taube and coworkers and Kirchner and coworkers have reported several studies on two-electron ($2e^-$) exchange reaction between the Ru^{II} and Ru^{IV} atoms in some mixed-valence halobiruthenocenium $(II,IV)^+Y^-$, ($[RcRcX]^+Y^-$: X = Cl, Br, I and Y = I_3, PF_6, BF_4) and mononuclear mixed systems of RcH/RcHX$^+$ and OcH/OcHX$^+$ by means of ^{1}H and ^{13}C-NMR spectroscopies [14–24]. All the results indicate that the migration of halogen atoms between the Ru^{II} in ruthenocene and the Ru^{IV} in haloruthenocenium is inevitable for the $2e^-$-exchange reaction. Considering these facts, the $2e^-$ transfer to the Ru^{IV} atom in $[RcHI]^+$ cation from the Ru^{II} atom in the [1.1]ferrocenylruthenocenophane is through a stable intermediate Ru^{IV}–I^- ··· Ru^{II} bridge, as shown in Scheme 2 (the stability of the Ru^{IV}–X^- bond increases in the order Cl < Br < I). This $2e^-$ transfer mechanism with $[RcHI]^+$ gives **3** not a monocationic ferrocenium cation **2**. Without such oxidation mechanisms with iodine, only Fe^{II} in [1.1]ferrocenylruthenocenophane is oxidized selectively with iodine giving a monocationic typical ferrocenium salt **2**. Ru^{II} in **2** was oxidized continuously with an excess of iodine giving a dicationic salt **1** with the Ru^{IV}–I^- bond. Actually, several attempts to prepare salt **3** using iodine only in various molar rations (neutral compound/I_2 = around 1/2–1/4) gave mixtures of **1** and **2**.

References

[1] M. Watanabe, I. Motoyama, T. Takayama, M. Shimoi and H. Sano *J. Organomet. Chem., 496* (1995) 87.

[2] U.T. Mueller-Westehoff, A.L. Rheingold and G.F. Swiegers, *Angew. Chem., Int. Ed. Engl., 31* (1992) 1353.

[3] A.L. Rheingold, U.T. Muller-Westerhoff, G.F. Swiegers and T.J. Haas, *Organometallics, 11* (1992) 3411.

[4] M. Watanabe and H. Sano, *Bull. Chem. Soc. Jpn., 63* (1990) 777.

[5] D.T. Cromer, J.T. Waber, *International Tables for X-ray Crystallography*, Vol. IV, Kynoch, Birmingham, UK, 1974, Table 2.2 A; J.A. Ibers and W.C. Hamilton, *Acta Crystallogr., 17* (1964) 781.

[6] D.C. Creagh, W.J. McAuley, *International Tables for X-ray Crystallography*, Vol. C, Kluwer Academic, Boston, 1992, Table 4.2.6.8, pp. 219–222.

[7] *TEXSAN: Crystal Structure Analysis Package*, Molecular Structure Corp., 1985.

[8] L. Pauling, *The Nature of the Chemical Bond*, 3rd edn., Cornell University Press, 1960.

[9] Y.S. Sone, A.W. Schlueter, D.N. Hendrickson and H.B. Gray, *Inorg. Chem., 13* (1974) 301.

[10] J.D. Dunitz, L.E. Orgel and A. Rich, *Acta Crystallogr., 9* (1956) 373.

[11] G.L. Hardrove and D.H. Templetom, *Acta Crystallogr., 12* (1959) 28.

[12] N.J. Mammano, A. Zalkin, A. Landers and A.L. Rheingold, *Inorg. Chem., 16* (1977) 297.

[13] M. Watanabe, I. Motoyama, M. Shimoi and T. Iwamoto, *Inorg. Chem., 33* (1994) 2518.

[14] M. Konno and H. Sano, *Bull. Chem. Soc. Jpn., 61* (1988) 1455; M.H. Delville, F. Robert, P. Gouzerh, J. Linares, K. Boukheddaden, F. Varret and D. Astruc, *J. Organomet. Chem., 451* (1993) C10; T.-Y. Dong, D.N. Hendrickson, K. Iwai, M.J. Cohn, S.J. Geib, A.L. Reingold, H. Sano, I. Motoyama and S. Nakasima, *107* (1985) 7996.

[15] M. Watanabe, T. Iwamoto, H. Sano and I. Motoyama, *J. Organomet. Chem., 446* (1993) 177.

[16] M. Watanabe, T. Iwamoto, A. Kuboi, S. Kawata, H. Sano and I. Motoyama, *Inorg. Chem., 31* (1992) 177.

[17] M. Watanabe, T. Iwamoto, H. Sano and I. Motoyama, *Inorg. Chem., 32* (1993) 5223.

[18] M. Watanabe, T. Iwamoto, H. Sano and I. Motoyama, *J. Organomet. Chem., 442* (1992) 309.

[19] M. Watanabe, I. Motoyama and H. Sano, *Inorg. Chim. Acta, 225* (1994) 103.

[20] T.P. Smith, D.J. Iverson, M.W. Droge, K.S. Kwan and H. Taube, *Inorg. Chem., 26* (1987) 2882.

[21] K. Kirchner, L.F. Han, H.W. Dodgen, S. Wherland and J.P. Hund, *Inorg. Chem., 29* (1990) 4556.

[22] K. Kirchner, H.W. Dodgen, S. Wherland and J.P. Hund, *Inorg. Chem., 28* (1989) 604.

[23] K. Kirchner, H.W. Dodgen, S. Wherland and J.P. Hund, *Inorg. Chem., 29* (1990) 2301.

[24] K. Kirchner, S.Q. Dang, M. Stebler, H.W. Dodgen, S. Wherland and J.P. Hund, *Inorg. Chem., 28* (1989) 3605.